

# Rendezvous and Docking of Co-Operative Target with Dual-Axis Gimbale Electric Thruster

Ankit M Patel<sup>1\*</sup> Vikram Kumar Saini<sup>2\*</sup> Aishashwini<sup>3\*</sup>  
Shashi Ranjan Kumar<sup>4\*\*</sup> Dipak Kumar Giri<sup>5\*</sup>

*\* Department of Aerospace Engineering, Indian Institute of Technology  
Kanpur, Uttar Pradesh - 208016, INDIA.*

*\*\* Department of Aerospace Engineering, Indian Institute of  
Technology Bombay, Maharashtra - 400076, INDIA.*

---

**Abstract:** This paper presents a simulation study on the feasibility of a dual-axis gimbale electric thruster for the relative orbital position control. Relative attitude of the spacecraft is controlled using reaction wheels (RWs). This study considers proportional derivative (PD) algorithm for orbital position control and nonlinear dynamic inversion for relative attitude control. The relative attitude dynamics is derived assuming that the target spacecraft is co-operative and is inactive, therefore, its relative attitude changes only due to its orbital motion around the central body. The dual-gimbal dynamics is approximated for control design due to coupling between gimbal rates. Numerical simulation results are presented for the showing the efficacy of the control algorithm as well the feasibility of the dual-axis gimbale thruster for relative orbital motion control.

*Keywords:* Rendezvous and Docking, Electric Thruster, Dual-axis Gimbal, Dynamic Inversion

---

## 1. INTRODUCTION

Autonomous rendezvous and docking (RVD) operations for spacecraft are some of the most crucial and challenging part of current space missions which includes on-orbit servicing of spacecraft, space structure assembly, transport vehicle approach and so on (Woffinden and Geller [2007]). Spacecraft rendezvous and docking refers to a technology in which two spacecrafts meet at the same position, velocity and time to unite and form a complex structure. RVD is performed with an active chaser spacecraft trying to capture a passive target spacecraft by adjusting its relative attitude and position towards target (Xie et al. [2021]). The RVD problem requires effective control of both relative position and relative attitude of the spacecrafts through some impulsive orbital maneuvers, detumbling and attitude corrections.

The actuator configuration selection for attitude and position control is a crucial problem particularly for missions that have tight constraints on total mass. For an RVD mission, the chaser spacecraft is subjected to significant impulsive forces, these forces may not pass through centre of gravity which results into significant rotation or tumbling of the spacecraft. For this reason high torque generation is also required. A vast amount of existing literature can be found about the RVD manoeuvres using impulsive thrust (Prussing [1970]), but

these impulsive thrusters use liquid propellant, which undesirably increases the spacecraft mass. Solar-powered electric thrusters reduce the total propellant mass for the mission requirement. These electric thrusters provide continuous low thrust compared to the conventional impulsive thrusters. Currently, research is being directed towards the case of rendezvous and docking manoeuvres of the chaser spacecraft with continuous thrust. Thrust vectoring is often used in space RVD by gimbaling the thrust produced by an electric thruster (Ma and Ghasemi Nejjhad [2005]); these thrust vectored manoeuvres are utilized to maintain the spacecraft trajectory. For future generation spacecrafts, thrust-vectoring spacecrafts are ideally suited due to their ability to reduce mass and volume. However, the low thrust provided by electric thrusters makes it infeasible to control the spacecraft's attitude by thruster vectoring. For attitude control mostly used actuators include magnetic rods, RWs and Variable Speed Control Moment Gyroscopes (VSCMGs). This paper uses the RWs as the primary actuator for attitude control, and dual-axis gimbale mechanism is adopted for the thrust vector control. We assume that the chaser spacecraft employs a series of separately operated continuous low-thrust electric actuators for rendezvous manoeuvring.

This paper aims to implement an autonomous RVD problem where a target spacecraft is moving in a known elliptic Keplerian orbit as shown in the Fig. (1). The chaser spacecraft approaches the target by firing a single electric thruster, which is considered to be mounted on a dual-axis gimbal mechanism providing thrust vectoring control as shown in the Fig. (2). Another set of two

---

\* <sup>1</sup> Under-Graduate Student

\*\*<sup>2</sup> Ph.D Student, Flight Mechanics and Control, vksaini.1997@gmail.com

\*<sup>3</sup>\*<sup>4</sup> Assistant Professor, srk@aero.iitb.ac.in

\*<sup>5</sup>\*<sup>6</sup> Assistant Professor, dkgiri@iitk.ac.in

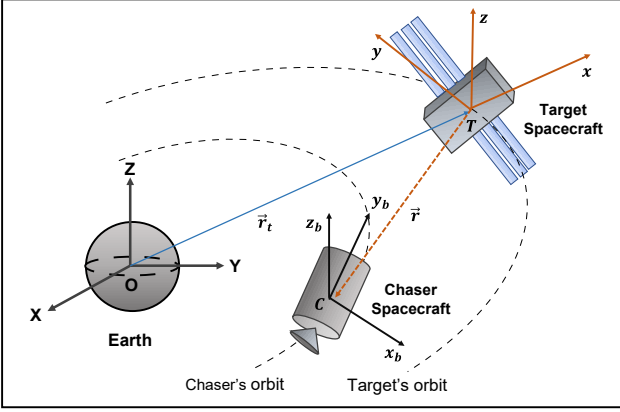


Fig. 1. Formation flying spacecrafts and their coordinate reference frame

auxiliary body-fixed cold gas thrusters is added to slow down the vehicle during the docking phase, since the main electric thruster is mounted at the back of the spacecraft as shown in the Fig. (3) and it is not possible to reverse the thrust due to mechanical constraints. For attitude control, a set of three RWs along three-body axes is mounted. The attitude dynamics is over actuated since the thrust vectoring of main electric thruster also provides net torque about centre of gravity of the vehicle. Main purpose of introducing the RWs is to cancel the thrust vectoring torque so that the thrust can be fired in a desired direction without affecting the attitude of the vehicle. Relative orbital motion is modelled for a generic Keplerian orbit under the influence of spherical gravity field. The relative distance between the spacecrafts is small as compared to the target orbit radius  $r_t$ , where the target orbit can be eccentric. Furthermore, the relative attitude motion is modelled by assuming that the target is cooperative and it's relative state information is available to chaser in real time with the help of the on-board sensors. It is supposed that the only change in target's attitude is due it's orbital motion. For controlling the relative position between the spacecrafts proportional derivative (PD) based control is used and for relative attitude control nonlinear dynamic inversion is used.

## 2. SPACECRAFT DYNAMICS MODELING

This section presents the modeling of the relative orbital motion, relative attitude dynamics between the two spacecrafts, and dual-axis gimbal mechanism motion.

### 2.1 Dual-Axis Gimballed Electric Thruster Model

A representation of the gimballed thruster is shown in Fig. (2), where the frame  $\mathcal{G}_o$  is attached to outer gimbal, where  $\hat{p}_1$ ,  $\hat{t}_1$  and  $\hat{g}_1$  are the unit vectors of frame  $\mathcal{G}_o$  with  $\hat{g}_1$  being outer gimbal axis and  $\gamma_1$  as it's gimbal angle, whereas frame  $\mathcal{G}_i$  corresponds to inner gimbal of the thruster, where  $\hat{p}_2$ ,  $\hat{t}_2$  and  $\hat{g}_2$  are the unit vectors of frame  $\mathcal{G}_i$  with  $\hat{g}_2$  being inner gimbal axis and  $\gamma_2$  as it's gimbal angle. The thrust obtained is always along  $\hat{t}_2$  unit vector. The relation between the units vector can be represented by

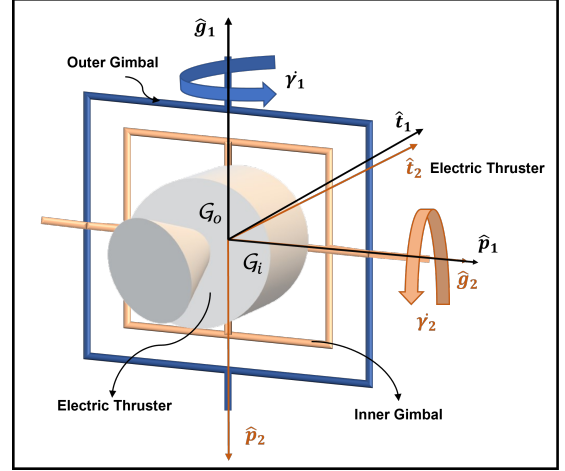


Fig. 2. Dual-axis gimballed Electric thruster

$$\begin{bmatrix} \hat{p}_1 \\ \hat{p}_1 \\ \hat{g}_1 \end{bmatrix} = \begin{bmatrix} \cos \gamma_1 & \sin \gamma_1 & 0 \\ -\sin \gamma_1 & \cos \gamma_1 & 0 \\ 0 & 0 & 1 \end{bmatrix} \begin{bmatrix} \hat{x}_b \\ \hat{y}_b \\ \hat{z}_b \end{bmatrix} \quad (1)$$

$$\begin{bmatrix} \hat{p}_2 \\ \hat{t}_2 \\ \hat{g}_2 \end{bmatrix} = \begin{bmatrix} 0 & \sin \gamma_2 & -\cos \gamma_2 \\ 0 & \cos \gamma_2 & \sin \gamma_2 \\ 1 & 0 & 0 \end{bmatrix} \begin{bmatrix} \hat{p}_1 \\ \hat{t}_1 \\ \hat{g}_1 \end{bmatrix} \quad (2)$$

Where,  $\hat{x}_b$ ,  $\hat{y}_b$  and  $\hat{z}_b$  are the basis vectors of the chaser's body frame  $\mathcal{B}$ , which will be discussed further in subsection (2.2.1) of this paper. Using the thrust vector  $\hat{t}_2$ , the thrust by the electric thruster is obtained by

$$T_{ET} = f \hat{t}_2$$

Where,  $f$  is the scalar thrust generated by electric thruster. Then thruster torque acting on a spacecraft can be obtained as

$$\tau_{ET} = f \rho \times \hat{t}_2$$

$$\tau_{ET} = f \begin{bmatrix} \rho_2 \sin \gamma_2 - \rho_3 \cos \gamma_2 \cos \gamma_1 \\ \rho_3 \cos \gamma_2 \sin \gamma_1 - \rho_1 \sin \gamma_2 \\ \rho_1 \cos \gamma_2 \cos \gamma_1 + \rho_2 \cos \gamma_2 \sin \gamma_1 \end{bmatrix} \quad (3)$$

Where,  $\rho = [\rho_1, \rho_2, \rho_3]^T$  is the position vector of  $C$  i.e., center of mass ( $c.m.$ ) of chaser spacecraft with respect to frame  $\mathcal{G}$  as shown in Fig.(3).

### 2.2 Relative Motion Model

**Coordinate reference frames** To describe the relative motion between the formation flying spacecrafts i.e., chaser and the target in a general Keplerian orbit, the following coordinate frames are illustrated in Fig. (1) and defined as

- $\mathcal{N} = OXYZ$  : the right-handed earth centered inertial frame, where the origin  $O$  is fixed at the center of the Earth, the  $\hat{X}$  and  $\hat{Z}$  basis vectors are directed towards sun i.e., vernal equinox and north pole respectively, whereas the  $\hat{Y}$  unit vector is chosen to complete the triad.
- $\mathcal{H} = Txyz$  : A cartesian right-handed frame is called Hill coordinate frame (Hill [1878]), where the origin  $T$  is fixed at the  $c.m.$  of target spacecraft, the  $\hat{x}$  is directed from the spacecraft radially outwards, while  $\hat{z}$  is parallel to the target's orbit momentum vector

in the orbit normal direction. The unit vector  $\hat{y}$  then completes the triad. This frame is also known as local-vertical-local-horizontal (LVLH) frame.

- $\mathcal{B} = Cx_b y_b z_b$  : A cartesian right-handed coordinate system attached to the chaser's c.m i.e  $C$  and it is called Body frame of chaser spacecraft.

In the remaining paper,  $\mathbf{S}^{\mathcal{N}}$  denotes the vector  $\mathbf{S}$  expressed in the frame  $\mathcal{N}$ , and  $\dot{\mathbf{S}}|_{\mathcal{N}}$  denotes the time derivative of vector  $\mathbf{S}$  in the frame  $\mathcal{N}$ .

**Relative Orbital Dynamics and Kinematics** Consider a relative motion of an active chaser spacecraft with respect to a passive target spacecraft in a general Keplerian orbit. The Hill (LVLH) frame is used to describe the relative motion. Thus, the relative position kinematical equation is given by

$$\dot{X} = V \quad (4)$$

Where,  $X = [x, y, z]^T$ ,  $V = [v_1, v_2, v_3]^T$  are the generalized relative position and velocity vectors of chaser spacecraft in  $\mathcal{H}$  frame.

The relative position dynamics between the chaser and the target in frame  $\mathcal{H}$  can be described using the following equations (Melton [2000], Schaub and Junkins [2014])

$$\ddot{x} - 2\omega_t \dot{y} - x\omega_t^2(1 + 2\frac{r_t}{p}) - y\dot{\omega}_t = a_x \quad (5)$$

$$\ddot{y} + 2\omega_t \dot{x} + x\dot{\omega}_t - y\omega_t^2(1 - \frac{r_t}{p}) = a_y \quad (6)$$

$$\ddot{z} + \frac{r_t}{p}\omega_t^2 z = a_z \quad (7)$$

Where,  $a_x$ ,  $a_y$  and  $a_z$  are control accelerations acting on the chaser spacecraft written in the target's frame  $\mathcal{H}$ ,  $\omega_t$  denotes the angular velocity vector of the rotating Hill frame  $\mathcal{H}$  relative to the inertial frame  $\mathcal{N}$  such that  $\omega_t = \dot{f}\hat{z}$ , with  $f$  being true anomaly of the target frame,  $p$  denotes parameter of orbit also known as semi-latus rectum. It is given by  $p = (1+e \cos f)/r_t$ , with  $e$  being eccentricity of the target's orbit, the scalar  $r_t > 0$  refer to the target's current orbit radius, and  $r = [x, y, z]^T$  represents the relative position vector of the chaser from the target in  $\mathcal{H}$  frame components.

In this paper, a near-range rendezvous scenario is considered. Thus for obtaining the above Eqs. (5), (6) and (7), an assumption is considered that the distance between the chaser and the target is much smaller as compared to the target's orbit radius, that is  $r_t \gg \|r\|$ . Eqs. (5), (6) and (7) can be reorganized into the general form as shown in Appendix B.

### Relative Rotational Dynamics and Kinematics

Using relative attitude quaternion  $q = \begin{bmatrix} q \\ q_4 \end{bmatrix} = [q_1, q_2, q_3, q_4]^T$  between  $\mathcal{H}$  and  $\mathcal{B}$  frame, with the constraint  $q^T q = 1$ , the relative attitude kinematical equation is given by

$$\dot{q} = \frac{1}{2}q \otimes \begin{bmatrix} \omega \\ 0 \end{bmatrix} = \frac{1}{2}\mathbf{S}(\omega)q \quad (8)$$

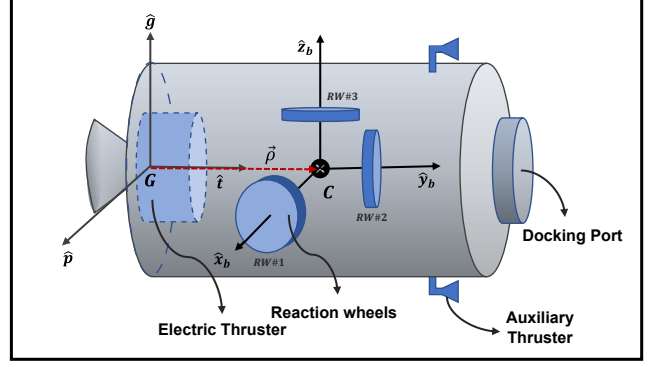


Fig. 3. Spacecraft model and actuator configuration

where,  $\omega = [\omega_1, \omega_2, \omega_3]^T$  is the relative angular velocity of chaser body frame  $\mathcal{B}$  with respect to Hill coordinate frame  $\mathcal{H}$  at target, and  $\mathbf{S}(\omega)$  is skew-symmetric matrix of  $\omega$ , which can be defined as

$$\mathbf{S}(\omega) = \begin{bmatrix} 0 & \omega_3 & -\omega_2 & \omega_1 \\ -\omega_3 & 0 & \omega_1 & \omega_2 \\ \omega_2 & -\omega_1 & 0 & \omega_3 \\ -\omega_1 & -\omega_2 & -\omega_3 & 0 \end{bmatrix} \quad (9)$$

The relative angular velocity can also be expressed as

$$\omega = \omega_c - R(q)\omega_t \quad (10)$$

Where,  $\omega_c = [\omega_{c1}, \omega_{c2}, \omega_{c3}]^T$  is the chaser's angular velocity with respect to inertial frame  $\mathcal{N}$  and expressed in frame  $\mathcal{B}$  i.e.,  $\omega_c = (\omega_{\mathcal{B}/\mathcal{N}})^{\mathcal{B}}$  and  $\omega_t$  is the target's angular velocity with respect to inertial frame  $\mathcal{N}$  and expressed in frame  $\mathcal{H}$  i.e.,  $\omega_t = (\omega_{\mathcal{H}/\mathcal{N}})^{\mathcal{H}}$  and  $R$  is the rotation matrix  $\mathbf{R}_{\mathcal{H}}^{\mathcal{B}} = R$ , transforming a vector from target's body frame  $\mathcal{H}$  to chaser's body frame  $\mathcal{B}$ , and can be expressed as

$$R = \begin{bmatrix} 2(q_1^2 + q_4^2) - 1 & 2(q_1q_2 + q_3q_4) & 2(q_1q_3 - q_2q_4) \\ 2(q_1q_2 - q_3q_4) & 2(q_2^2 + q_4^2) - 1 & 2(q_2q_3 + q_1q_4) \\ 2(q_1q_3 + q_2q_4) & 2(q_2q_3 - q_1q_4) & 2(q_3^2 + q_4^2) - 1 \end{bmatrix} \quad (11)$$

Differentiating Eq.(10) yields

$$\dot{\omega}|_{\mathcal{N}} = \dot{\omega}_c|_{\mathcal{N}} - R(q)(\dot{\omega}_t|_{\mathcal{N}})^{\mathcal{H}} \quad (12)$$

Furthermore using transport theorem Eq.(12) leads to

$$\dot{\omega}|_{\mathcal{H}} + \omega_t \times \omega = \dot{\omega}_c|_{\mathcal{N}} - R(q)(\dot{\omega}_t|_{\mathcal{N}})^{\mathcal{H}} \quad (13)$$

Where, all the above entities in Eq. (13) are expressed in target's body frame  $\mathcal{H}$ .

For the chaser spacecraft, the attitude dynamics  $\dot{\omega}_c|_{\mathcal{N}}$  is derived from the conservation of angular momentum  $h$  i.e.,

$$\dot{h}|_{\mathcal{N}} = 0 \quad (14)$$

Considering all the momentum storage elements of the active chaser spacecraft, the total angular momentum  $h$  of chaser spacecraft in frame  $\mathcal{B}$  is expressed as follows

$$h = h_b + h_{og} + h_{ig} + h_{RW}$$

$$h = J\omega_c + I_{og}\dot{\gamma}_1\hat{g}_1 + I_{ig}\dot{\gamma}_2\hat{g}_2 + h_{RW} \quad (15)$$

Where,  $h_b$  is angular momentum of chaser spacecraft body,  $h_{og}$  and  $h_{ig}$  are angular momentum of outer gimbal and inner gimbal respectively and  $J \in \mathbb{R}^{3 \times 3}$  is the inertia matrix of the chaser spacecraft,  $I_{og}$  and  $I_{ig}$  are the inertia of the outer gimbal and inner gimbal along their respective gimbal axes,  $h_{RW}$  is the angular momentum of the reaction wheels in frame  $\mathcal{B}$ , that is

$$h_{RW} = I_{RW}\Omega = \begin{bmatrix} I_1 & 0 & 0 \\ 0 & I_2 & 0 \\ 0 & 0 & I_3 \end{bmatrix} \begin{bmatrix} \Omega_1 \\ \Omega_2 \\ \Omega_3 \end{bmatrix}$$

The differentiation of Eq. (15) leads to the following equation

$$\dot{h}|_{\mathcal{B}} = J\dot{\omega}_c + I_{ig}\dot{\gamma}_2\hat{g}_2 + \dot{h}_{RW} \quad (16)$$

Here, with the assumption that the inertia matrix  $J$  is constant yields  $\dot{J} = 0$ , the effect of the terms  $\dot{\gamma}_1$ ,  $\dot{\gamma}_2$  are also assumed to be negligible as justified in (Yoon and Tsiotras [2006]) and  $\dot{h}_{RW}$  is given by

$$\dot{h}_{RW} = I_{RW}\dot{\Omega} = \begin{bmatrix} I_1 & 0 & 0 \\ 0 & I_2 & 0 \\ 0 & 0 & I_3 \end{bmatrix} \begin{bmatrix} \dot{\Omega}_1 \\ \dot{\Omega}_2 \\ \dot{\Omega}_3 \end{bmatrix} \quad (17)$$

Putting Eq. (16) in terms of the basis vectors of  $\mathcal{B}$  frame using Eq. (1) and (2) yields

$$\begin{aligned} \dot{h}|_{\mathcal{B}} = & J\dot{\omega}_c + (-I_{ig}\dot{\gamma}_1\dot{\gamma}_2 \sin \gamma_1 + I_1\dot{\Omega}_1)\hat{x}_b + \dots \\ & + (I_{ig}\dot{\gamma}_1\dot{\gamma}_2 \cos \gamma_1 + I_2\dot{\Omega}_2)\hat{y}_b + (I_3\dot{\Omega}_3)\hat{z}_b \end{aligned} \quad (18)$$

The coupled non-linear terms of  $\dot{\gamma}_1\dot{\gamma}_2$  are not used in the control allocation in this paper. The control allocation is done using Eq. (21). From the transport theorem, the inertial derivative of Eq. (15) is related to Eq.(18) as follows

$$\dot{h}|_{\mathcal{N}} = \dot{h}|_{\mathcal{B}} + \omega_c \times h \quad (19)$$

Using Eqs. (15), (18) and (19) yields the rotational dynamics of chaser spacecraft as

$$J\dot{\omega}_c = U - \omega_c \times (I_{RW}\Omega + J\omega_c) + \tau_{EP} \quad (20)$$

Where,  $\tau_{EP}$  is the electric thruster torque acting about point  $C$  of chaser spacecraft as calculated in Eq. (3) and  $U$  is the control torque given by the following equation considering  $C\gamma = \cos(\gamma)$  and  $S\gamma = \sin(\gamma)$

$$U = \begin{bmatrix} -I_1 & 0 & 0 \dots \\ -I_{og}\omega_{c_2} & I_{ig}\omega_{c_3}S\gamma_1 & \\ 0 & -I_2 & 0 \dots \\ I_{og}\omega_{c_1} & -I_{ig}\omega_{c_3}C\gamma_1 & \\ 0 & 0 & -I_3 \dots \\ 0 & I_{ig}(\omega_{c_2}C\gamma_1 - \omega_{c_1}S\gamma) & \end{bmatrix}^{3 \times 5} \begin{bmatrix} \dot{\Omega}_1 \\ \dot{\Omega}_2 \\ \dot{\Omega}_3 \\ \dot{\gamma}_1 \\ \dot{\gamma}_2 \end{bmatrix} \quad (21)$$

Where,  $\dot{\Omega}_1$ ,  $\dot{\Omega}_2$ ,  $\dot{\Omega}_3$ ,  $\dot{\gamma}_1$  and  $\dot{\gamma}_2$  are the control inputs of reaction wheels and gimbals. Now using Eq. (13) and (20), the relative rotational dynamics is derived as follows

$$\dot{\omega} = J^{-1}(U - \omega_c \times (I_{RW}\Omega + J\omega_c) + \tau_{EP}) + \dots - \omega_t \times \omega - R(q)\dot{\omega}_t \quad (22)$$

In the above equation few superscript and subscript are omitted for clarity. Thus, the relative attitude dynamics has been derived.

### 3. QUATERNION ERROR DYNAMICS

Let us define a unit error quaternion  $q_e = \begin{bmatrix} q_e \\ q_{e_4} \end{bmatrix} = [q_{e_1}, q_{e_2}, q_{e_3}, q_{e_4}]^T$  as (Parwana et al. [2018])

$$q = q_d \otimes q_e$$

$$q_e = \bar{q}_d \otimes q \quad (23)$$

where,  $q_d = [q_{d_1}, q_{d_2}, q_{d_3}, q_{d_4}]^T$  be the desired relative attitude quaternion and  $\bar{q}_d$  denotes its conjugate i.e.,  $\bar{q}_d = [-q_{d_1}, -q_{d_2}, -q_{d_3}, q_{d_4}]^T$ . Thus, differentiating the above Eq. (23), the error kinematics equation is derived as

$$\dot{q}_e = \bar{q}_d \otimes (\dot{q} - \dot{q}_d \otimes q_e) \quad (24)$$

Using Eq. (8) for  $q$  and  $q_d$ , the Eq.(24) leads to

$$\dot{q}_e = \frac{1}{2}q_e \otimes (\mathbf{w} - \bar{q}_e \otimes \mathbf{w}_d^{\mathcal{D}} \otimes q_e) \quad (25)$$

Where,  $\mathbf{w}$  is the relative angular velocity quaternion i.e.,  $\mathbf{w} = \begin{bmatrix} \omega \\ 0 \end{bmatrix}$  and  $\mathbf{w}_d^{\mathcal{D}}$  is the desired angular velocity quaternion in desired quaternion frame  $\mathcal{D}$  such that  $\mathbf{w}_d^{\mathcal{D}} = q_e \otimes \mathbf{w}_d^{\mathcal{H}} \otimes \bar{q}_e$  where  $\mathcal{H}$  denotes Hill coordinate frame. As in this paper a RVD scenario is considered. Thus, the desired relative attitude quaternion  $q_d = [0, 0, 0, 1]^T$  and constant. Hence, Eq. (25) yields

$$\dot{q}_e = \frac{1}{2}q_e \otimes \mathbf{w} = \frac{1}{2}\mathbf{S}(\omega)q_e \quad (26)$$

Differentiating Eq. (26) yields the quaternion error dynamics as follows

$$\ddot{q}_e = \frac{1}{2}G^T\dot{\omega} \quad (27)$$

Where, the matrix  $G$  is defined as

$$G = \begin{bmatrix} q_{e_4} & q_{e_3} & -q_{e_2} & -q_{e_1} \\ -q_{e_3} & q_{e_4} & q_{e_1} & -q_{e_2} \\ q_{e_2} & -q_{e_1} & q_{e_4} & -q_{e_3} \end{bmatrix}$$

### 4. CONTROL LAW DESIGN

#### 4.1 Spacecraft attitude control

In this subsection, we design controller for spacecraft attitude control based on dynamic inversion. We formulate

the relative attitude control by imposing a second order error stabilizing dynamics to achieve the desired attitude i.e.,  $q_d = [0, 0, 0, 1]^T$  which is also the equilibrium point for the error quaternion and corresponds to perfect overlap of target and chaser frames. The second order error dynamics can be written as

$$\ddot{q}_e + 2\zeta\omega_n\dot{q}_e + \omega_n^2(q_e - q_d) = 0 \quad (28)$$

Where,  $q_e$  is the unit error quaternion,  $\zeta$  and  $\omega_n$  are the design parameters which are generally called damping ratio and natural frequency respectively. Putting  $\ddot{q}_e$ ,  $\dot{q}_e$  from Eq. (27) and Eq. (26) the above equation i.e., Eq. (28) leads to

$$\dot{\omega} = G(-2\zeta\omega_n(\mathbf{S}(\omega)q_e) - 2\omega_n^2(q_e - q_d)) \quad (29)$$

Equating Eq. (29) with Eq. (22) gives the control torque  $U$  as follows

$$U = J(-2G(\zeta\omega_n(\mathbf{S}(\omega)q_e) + \omega_n^2(q_e - q_d)) + \omega_t \times \omega + \dots + R(q)\dot{\omega}_t) + \omega_c \times (I_{RW}\Omega + J\omega_c) - \tau_{ET} \quad (30)$$

*Stability Analysis* The proof of Lyapunov stability for the control law  $U$  is given in Appendix A.

#### 4.2 Spacecraft position control

For the relative position control PD control law is implemented as follows

$$T = -k_1X - k_2\dot{X}$$

Where,  $a = [a_x, a_y, a_z]^T$  is the control accelerations by thrusters,  $X = [x, y, z]^T$  is the relative position vector, here  $k_1$  and  $k_2$  are the design parameters of the controller generally called as proportional and derivative gains. Using the relative position kinematical equation from Eq. (4), the above equation yields

$$T = -k_1X - k_2V \quad (31)$$

Where,  $V$  is the relative velocity vector. From Eq. (B.6) and (11),  $T$  in the Hill frame can be written as  $T = R(q)^{-1}T_{\mathcal{B}}$ , using this relation in the Eq. (31) yields

$$T_{\mathcal{B}} = R(q)(-k_1X - k_2V) \quad (32)$$

Where, the thrust  $T_{\mathcal{B}} = [a_{x_{\mathcal{B}}}, a_{y_{\mathcal{B}}}, a_{z_{\mathcal{B}}}]^T$  is allocated among the electric thruster and auxiliary thruster such that if  $a_{y_{\mathcal{B}}} < 0$  then the  $T_{aux} = a_{y_{\mathcal{B}}}$  and then corresponding thrust from electric thruster i.e.,  $f = \sqrt{a_{x_{\mathcal{B}}}^2 + a_{z_{\mathcal{B}}}^2}$  is allocated. But if  $a_{y_{\mathcal{B}}} > 0$  then simply  $T_{aux} = 0$  and  $f = \sqrt{a_{x_{\mathcal{B}}}^2 + a_{y_{\mathcal{B}}}^2 + a_{z_{\mathcal{B}}}^2}$ . Here for chaser's position control,  $T_{aux}$  and  $f$  are control inputs.

## 5. NUMERICAL SIMULATION

In this section, we provide numerical simulations for the formation flying spacecraft i.e., the chaser and target

Parameters	Value
Orbit type	Keplerian
Semi-major axis (m)	6786000
Eccentricity	0.01
Inclination (deg)	50
Right ascension of the ascending node (deg)	90
Argument of periasis (deg)	93
True anomaly (deg)	203

Table 1. Orbit parameters of the target spacecraft

Parameter	Value
$M_{chaser}$	80 (Kg)
$J$	$diag\{25.416, 10, 25.416\}$ (Kg.m <sup>2</sup> )
$I_{ig}$	0.30 (Kg.m <sup>2</sup> )
$I_{og}$	0.32 (Kg.m <sup>2</sup> )
$I_{RW}$	$diag\{0.05, 0.05, 0.05\}$ (Kg.m <sup>2</sup> )
$\omega_n$	0.133
$\zeta$	0.707
$k_1$	$0.1118 \times 10^{-4}$
$k_2$	$0.33 \times 10^{-2}$
$\rho$	$[0, 0.15, 0]^T$ (m)

Table 2. Simulation parameters

Quantity	Initial conditions
Quaternion	$[0.1826, -0.3651, -0.5477, 0.7303]^T$
Angular Velocity (rad/s)	$[0, 0, 0.1]^T$
Position (m)	$[1000, 500, 500]^T$
Velocity (m/s)	$[0, 0, 0]^T$

Table 3. Initial conditions for numerical simulation

spacecraft for an autonomous RVD with parameters as provided in Table 1. Initial conditions for simulation are provided in Table 3. Other simulation parameters such as weight of active spacecraft, inertial matrix and values for spacecraft, reactions wheels and gimbal are provided in Table 2.

#### 5.1 Relative Attitude Control

For relative attitude control desired quaternion is  $q_d = [0, 0, 0, 1]^T$ , in case of a rendezvous and docking problem, this implies the full attitude synchronization of chaser and target spacecraft is to be achieved. The results for attitude synchronization along with its control requirements are shown in Fig. (4). It is observed that the quaternion approaches to the desired value in  $t = 200$  seconds. The attitude control parameters also saturates at about  $t = 200$  seconds.

#### 5.2 Relative Position Control

Desired relative position of target with respect to chaser is zero. The results for the spacecraft rendezvous and the thrust requirement are shown in Fig. (5). It is observed that the position and velocity approaches zero within  $t = 2400$  seconds and the maximum thrust required from electric thruster and auxiliary thruster are found out to be 10 N and 5 N respectively.

## 6. CONCLUSION

This paper presented rendezvous and docking to a target spacecraft using PD control for relative orbital position

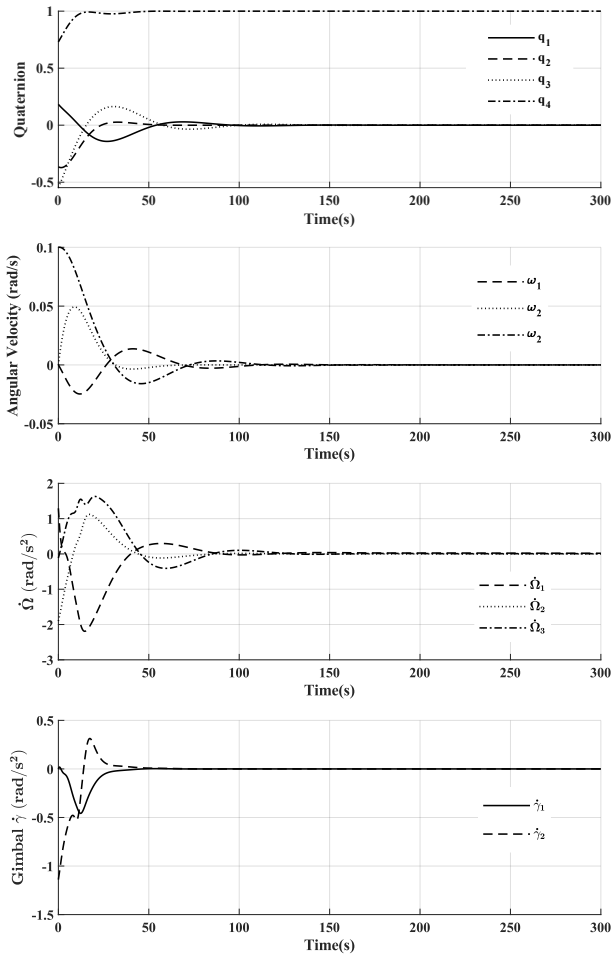


Fig. 4. Attitude stabilization of chaser spacecraft

control and nonlinear dynamic inversion for relative attitude control. The commanded thrust force is found to be higher than feasible limits of existing electric thruster technology if one individual thruster is used, but in conjunction with multiple parallel thrusters, it is possible to achieve the commanded thrust. Commanded torque is found to be within the achievable limits of RWs. The attitude control law was formulated with some approximation on coupling terms of gimbal rates which can be considered in a future study without approximation. Optimal allocation of torque among the RWs and electric thruster generated torque can also be studied as future work.

#### REFERENCES

- Hill, G.W. (1878). Researches in the lunar theory. *American Journal of Mathematics*, 1(1), 5–26. URL <http://www.jstor.org/stable/2369430>.
- Khalil, H. (1996). Nonlinear systems, printice-hall. *Upper Saddle River, NJ*, 3.
- Ma, K. and Ghasemi Nejhada, M. (2005). Precision positioning of a parallel manipulator for spacecraft thrust vector control. *Journal of Guidance Control and Dynamics - J GUID CONTROL DYNAM*, 28, 185–188. doi:10.2514/1.11112.
- Melton, R.G. (2000). Time-explicit representation of relative motion between elliptical orbits. *Journal of*

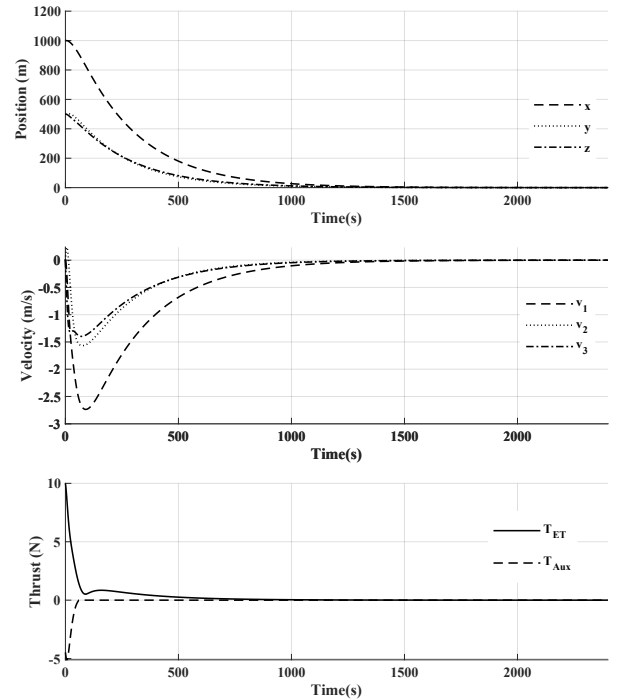


Fig. 5. Position stabilization of chaser spacecraft

- Guidance, Control, and Dynamics*, 23(4), 604–610. doi:10.2514/2.4605.
- Parwana, H., Patrikar, J.S., and Kothari, M. (2018). A Novel Fully Quaternion based Nonlinear Attitude and Position Controller. doi:10.2514/6.2018-1587.
- Prussing, J.E. (1970). Optimal two- and three-impulse fixed-time rendezvous in the vicinity of a circular orbit. *AIAA Journal*, 8(7), 1221–1228. doi:10.2514/3.5876.
- Schaub, H. and Junkins, J. (2014). *Analytical Mechanics of Space Systems*. AIAA education series. American Institute of Aeronautics and Astronautics, Incorporated.
- Slotine, J.J.E., Li, W., et al. (1991). *Applied nonlinear control*, volume 199. Prentice hall Englewood Cliffs, NJ.
- Woffinden, D.C. and Geller, D.K. (2007). Navigating the road to autonomous orbital rendezvous. *Journal of Spacecraft and Rockets*, 44(4), 898–909.
- Xie, Y., Chen, C., Liu, T., and Wang, M. (2021). *Guidance, Navigation, and Control for Spacecraft Rendezvous and Docking: Theory and Methods*. Springer Nature.
- Yoon, H., Eun, Y., and Park, C. (2014). Adaptive tracking control of spacecraft relative motion with mass and thruster uncertainties. *Aerospace Science and Technology*, 34, 75–83.
- Yoon, H. and Tsiotras, P. (2006). Spacecraft line-of-sight control using a single variable-speed control moment gyro. *Journal of guidance, control, and dynamics*, 29(6), 1295–1308.

#### Appendix A. STABILITY ANALYSIS

Considering the stable second order error dynamics (Slotine et al. [1991]) as given in Eq. (28), assures our control input to be exponentially stable. For the global stability of the control input, a Lyapunov stability analysis is provided with a Lyapunov candidate function as (Parwana et al. [2018])

$$V = \delta \mathbf{q}_e^T \mathbf{q}_e + \delta(1 - q_{e_4})^2 + \frac{1}{2} \omega^T J \omega^T$$

$$V = 2\delta(1 - q_{e_4}) + \frac{1}{2} \omega^T J \omega^T \quad (\text{A.1})$$

Where  $\delta > 0$  is a constant and  $\mathbf{q}_e$  is vector part of the error quaternion. Differentiating Eq.(A.1) yields the derivative of Lyapunov function such as

$$\dot{V} = -2\delta \dot{q}_{e_4} + \omega^T J \dot{\omega}$$

It should be noted that  $\omega^T J \dot{\omega} = \omega^T J \dot{\omega}^T$  as both are scalar and equal. Using Eq.(26),  $\dot{q}_{e_4}$  is obtained as  $\dot{q}_{e_4} = -\frac{1}{2} \mathbf{q}_e \cdot \omega = -\frac{1}{2} \mathbf{q}_e^T \omega$  and substituting  $\dot{\omega}$  from Eq.(29) yields

$$\dot{V} = \delta \mathbf{q}_e^T \omega - 2\omega^T J G(\zeta \omega_n \dot{q}_e + \omega_n^2 (q_e - q_d))$$

Using the relations  $q_e \otimes \mathbf{w} = G^T \omega$  and  $G G^T = I$ . The above equation can be formulated as

$$\dot{V} = \delta \mathbf{q}_e^T \omega - 2\omega^T J \zeta \omega_n \omega - 2\omega^T J G \omega_n^2 (q_e - q_d)$$

$$\dot{V} = \delta \mathbf{q}_e^T \omega - 2\omega^T J \zeta \omega_n \omega - 2\omega^T J \omega_n^2 \mathbf{q}_e \quad (\text{A.2})$$

where we have used the relation that  $G(q_e - q_d) = \mathbf{q}_e$  as  $G q_e = \mathbf{0}_{3 \times 1}$ . Now, taking  $\delta = 2J \omega_n^2$  such that the Eq.(A.2) formulates to

$$\dot{V} = -2\zeta \omega_n \omega^T J \omega^T \quad (\text{A.3})$$

Thus, the above expression concludes that  $\dot{V}$  is negative semi-definite. Using boundness of the input parameters and differentiating above equation i.e., Eq. (A.3), the boundedness of  $\ddot{V}$  can be easily shown and thus uniform continuity of  $\dot{V}$  is assured. Hence, the proof that  $\dot{V} \rightarrow 0$  as  $t \rightarrow \infty$  and global asymptotic stability of  $\omega$  can be proved by Barbalat's lemma (Khalil [1996]), which also implies that  $\|\dot{\omega}\| \rightarrow 0$  as  $t \rightarrow \infty$  for our mission scenario. Now considering the dynamic equation from Eq. (29) and Eq. (26), it can be formulated as

$$\dot{\omega} = G(-2\zeta \omega_n (q_e \otimes \omega) - 2\omega_n^2 (q_e - q_d))$$

Using similar steps as in formulation of  $\dot{V}$  the above expression can be written as

$$\dot{\omega} = -2\zeta \omega_n \omega - \omega_n^2 \mathbf{q}_e$$

This can be further rearranged as

$$\|\omega_n^2 \mathbf{q}_e\| = \|-\dot{\omega} - 2\zeta \omega_n \omega\|$$

$$\|\omega_n^2 \mathbf{q}_e\| \leq \|\dot{\omega}\| + \|2\zeta \omega_n \omega\|$$

Using the global asymptotic stability of  $\omega$ , all the terms at right hand side falls to zero as  $t \rightarrow \infty$ . Thus,  $\|\mathbf{q}_e\| \rightarrow 0$  which implies that  $q_{e_4} \rightarrow \pm 1$ . The asymptotic stable property of  $q_{e_4} = 1$  can be assured by selecting a proper value of  $\delta$  (Parwana et al. [2018]). Hence, the system is therefore global asymptotically stable.

## Appendix B. GENERAL FORM FOR RELATIVE ORBITAL MOTION

$$L\ddot{X} + M\dot{X} + NX = T \quad (\text{B.1})$$

where,  $L \in \mathbb{R}^{3 \times 3}$  is the inertia matrix which is symmetric and positive definite,  $M\dot{X}$  represents the Coriolis effect and centrifugal force,  $NX$  represents gravitational force, and  $T$  is the control input vector. These system matrices for the relative dynamics are given as (Yoon et al. [2014])

$$L = \begin{bmatrix} 1 & 0 & 0 \\ 0 & 1 & 0 \\ 0 & 0 & 1 \end{bmatrix} \quad (\text{B.2})$$

$$M = \begin{bmatrix} 0 & -2\omega_t & 0 \\ 2\omega_t & 0 & 0 \\ 0 & 0 & 0 \end{bmatrix} \quad (\text{B.3})$$

$$N = \begin{bmatrix} -\omega_t^2(1 + 2\frac{r_t}{p}) & -\dot{\omega}_t & 0 \\ \dot{\omega}_t & -\omega_t^2(1 - \frac{r_t}{p}) & 0 \\ 0 & 0 & \omega_t^2 \frac{r_t}{p} \end{bmatrix} \quad (\text{B.4})$$

$$T = [a_x, a_y, a_z]^T \quad (\text{B.5})$$

As the chaser is an active spacecraft, we have the control accelerations in the chaser's body frame  $\mathcal{B}$ . Hence, let  $T_{\mathcal{B}} = [a_{x_{\mathcal{B}}}, a_{y_{\mathcal{B}}}, a_{z_{\mathcal{B}}}]^T$  be the control accelerations by the chaser's thrusters expressed in the  $\mathcal{B}$  frame. Its relation with the control input in  $\mathcal{H}$  i.e.,  $T$  and is given as

$$T = \mathbf{R}_{\mathcal{B}}^{\mathcal{H}} T_{\mathcal{B}} \quad (\text{B.6})$$

where,  $\mathbf{R}_{\mathcal{B}}^{\mathcal{H}}$  is the rotation matrix, transforms a vector from frame  $\mathcal{B}$  to frame  $\mathcal{H}$ . Thus, substituting the above equation, Eq. (B.6) in Eq. (B.1) leads to the final generalized form of the relative position dynamics as follows

$$L\ddot{X} + M\dot{X} + NX = \mathbf{R}_{\mathcal{H}}^{\mathcal{B}} T_{\mathcal{B}} \quad (\text{B.7})$$

where,  $\mathbf{R}_{\mathcal{H}}^{\mathcal{B}} = (\mathbf{R}_{\mathcal{B}}^{\mathcal{H}})^{-1}$  and has been evaluated in as Eq. (11).